nature biotechnology

Resolution of liver cirrhosis using vitamin A–coupled liposomes to deliver siRNA against a collagen-specific chaperone

Yasushi Sato[1,2], Kazuyuki Murase[1,2], Junji Kato[1,2], Masayoshi Kobune[1], Tsutomu Sato[1], Yutaka Kawano[1], Rishu Takimoto[1], Kouichi Takada[1], Koji Miyanishi[1], Takuya Matsunaga[1], Tetsuji Takayama[1] & Yoshiro Niitsu[1]

There are currently no approved antifibrotic therapies for liver cirrhosis. We used vitamin A–coupled liposomes to deliver small interfering RNA (siRNA) against gp46, the rat homolog of human heat shock protein 47, to hepatic stellate cells. Our approach exploits the key roles of these cells in both fibrogenesis as well as uptake and storage of vitamin A. Five treatments with the siRNA-bearing vitamin A–coupled liposomes almost completely resolved liver fibrosis and prolonged survival in rats with otherwise lethal dimethylnitrosamine-induced liver cirrhosis in a dose- and duration-dependent manner. Rescue was not related to off-target effects or associated with recruitment of innate immunity. Receptor-specific siRNA delivery was similarly effective in suppressing collagen secretion and treating fibrosis induced by CCl_4 or bile duct ligation. The efficacy of the approach using both acute and chronic models of liver fibrosis suggests its therapeutic potential for reversing human liver cirrhosis.

Liver cirrhosis, or fibrosis, the ultimate pathological feature of all forms of chronic hepatic damage, is responsible for much morbidity and mortality worldwide. The principal cell type responsible for liver fibrosis is the hepatic stellate (HS) cell, a resident perisinusoidal cell that takes up vitamin A from circulation and stores it. When stimulated by reactive oxygen intermediates or cytokines, HS cells become activated and are transformed to proliferative, fibrogenic and contractile myofibroblasts[1], which synthesize and secrete procollagen, which accumulates as insoluble collagen after its terminal domains are cleaved by procollagen peptides, causing fibrosis. The collagen-specific chaperone, heat shock protein 47 (HSP47), facilitates collagen secretion by ensuring proper triple-helix formation of procollagen in the endoplasmic reticulum and has also been implicated in translational regulation of procollagen synthesis[2,3].

The demonstration that liver fibrosis in animals[4] and humans[5] can regress when collagen synthesis is inhibited suggests that fibrosis can be reversed, most likely by the activity of matrix metalloproteinases. Various therapeutic approaches to inhibit collagen synthesis or activate matrix metalloproteinases have been investigated in animal models[6,7]. However, none have yet been applied clinically, mainly because of side effects resulting from an inability to specifically target particular molecules and/or cells.

The specific association of HSP47 with a diverse range of collagen types[3,8,9] makes it an excellent candidate for targeting HS cell–mediated collagen secretion using siRNA. To enhance the specificity of such a strategy, we reasoned that encapsulating the siRNA in vitamin A–coupled liposomes should target it preferentially to HS cells, which have a remarkable capacity for vitamin A uptake, most likely through receptors for retinol binding protein (RBP).

Using three animal models of liver cirrhosis—involving induction by dimethylnitrosamine (DMN), CCl_4 or bile duct ligation—our histological analysis shows that intravenous (i.v.) injection of vitamin A–coupled liposomes carrying siRNA against mRNA encoding rat gp46, a homolog of HSP47, (VA-lip-siRNAgp46), rapidly resolves liver fibrosis. As cells analogous to HS cells apparently play an essential role in causing fibrosis associated with chronic pancreatitis[10] and laryngeal fibrosis[11], our approach may find value in treating fibrotic conditions in organs besides the liver.

RESULTS

siRNAgp46 suppresses gp46 expression and collagen secretion

We first elucidated the effects of three siRNAs (types A, B, C) on the abundance of gp46 transcripts (**Fig. 1a** and **Supplementary Fig. 1** online) in normal rat kidney (NRK) cells, previously used to study collagen production[12]. All three siRNAs suppressed accumulation of gp46 mRNA (**Supplementary Fig. 1b**) and gp46 protein (**Fig. 1a**), but the greatest efficacy, observed using type A siRNA (siRNAgp46A), led us to select it for subsequent experiments. Transducing NRK cells with various dosages of siRNAgp46A revealed an apparent dose-dependent suppression of gp46 expression with almost complete suppression at 50 nM (**Fig. 1b**). We then used proline incorporation assays to test whether siRNAgp46A could inhibit collagen secretion. The concentration of newly synthesized collagen in the culture medium of NRK cells

[1]Fourth Department of Internal Medicine, Sapporo Medical University, School of Medicine, Sapporo, 060-8543, Japan. [2]These authors contributed equally to this work. Correspondence should be addressed to Y.N. (niitsu@sapmed.ac.jp).

Received 27 January; accepted 6 March; published online 30 March 2008; doi:10.1038/nbt1396

transduced with siRNAgp46A was significantly reduced compared with parental cells and cells transfected with randomly selected siRNAs (siRNArandom) ($P < 0.01$) (**Fig. 1c**). Collagen secretion from cultured NRK cells was measured by Sirius red dye binding and spectrophotometry[13]. Significantly less collagen was secreted by siRNAgp46A-treated NRK cells than by non-treated NRK or NRK cells treated with siRNArandom ($P < 0.01$) (**Fig. 1d**).

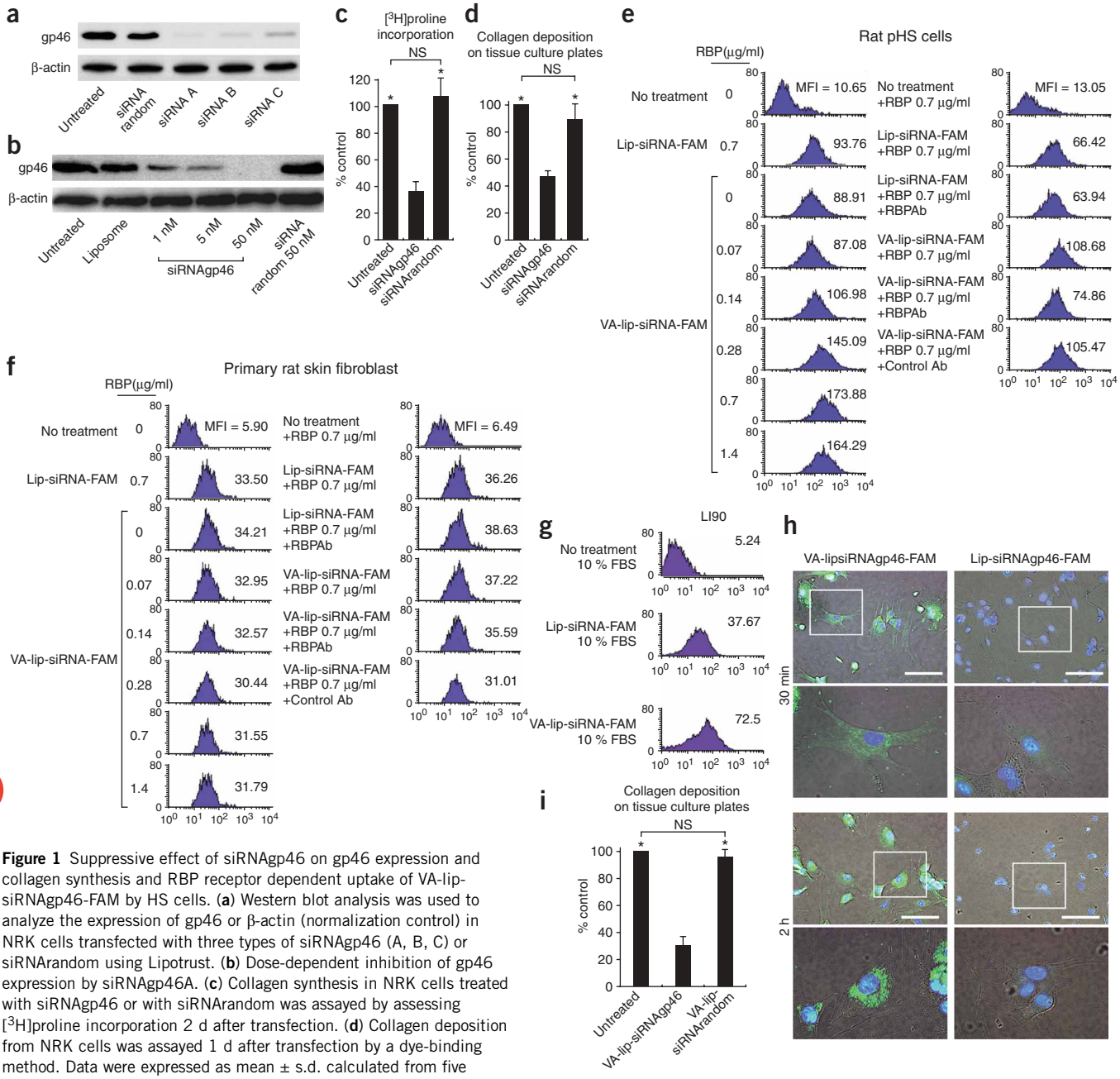

Figure 1 Suppressive effect of siRNAgp46 on gp46 expression and collagen synthesis and RBP receptor dependent uptake of VA-lip-siRNAgp46-FAM by HS cells. (**a**) Western blot analysis was used to analyze the expression of gp46 or β-actin (normalization control) in NRK cells transfected with three types of siRNAgp46 (A, B, C) or siRNArandom using Lipotrust. (**b**) Dose-dependent inhibition of gp46 expression by siRNAgp46A. (**c**) Collagen synthesis in NRK cells treated with siRNAgp46 or with siRNArandom was assayed by assessing [^{3}H]proline incorporation 2 d after transfection. (**d**) Collagen deposition from NRK cells was assayed 1 d after transfection by a dye-binding method. Data were expressed as mean ± s.d. calculated from five transfections and as a percentage of untreated control. *$P < 0.01$ versus siRNAgp46. NS, not significant. (**e,f**) Representative FACS patterns of rat pHS cell (**e**) and primary rat skin fibroblast (**f**) treated with vitamin A-free liposomes carrying siRNAgp46-FAM (lip-siRNAgp46-FAM) or VA-lip-siRNAgp46-FAM in the presence of various concentrations (0.07–1.4 μg/ml) of RBP and of the cells treated with lip-siRNAgp46-FAM or VA-lip-siRNAgp46-FAM in 0.7 μg/ml RBP with or without anti-RBP antibody. Irrelevant mouse monoclonal antibody served as a negative control. (**g**) Representative FACS patterns of LI90 cells treated with lip-siRNAgp46-FAM or VA-lip-siRNAgp46-FAM in the presence of 10% FBS. Mean fluorescence intensity (MFI) is indicated. Five independent experiments were carried out in each of (**e–g**), and the results were essentially the same. (**h**) Representative fluorescent images of the intracellular distribution of FAM-labeled siRNA. Rat pHS cells were treated with VA-lip-siRNAgp46-FAM or lip-siRNAgp46-FAM. At 30 min, the medium was replaced with fresh medium. At the time indicated, cells were fixed and analyzed by fluorescence microscopy to determine the relative intracellular distribution of the siRNA-FAM (green). Pictures taken at original magnification (× 200, upper panel) and magnified images corresponding to the areas enclosed in boxes are presented in lower panel. Scale bars, 100 μm. One representative image of five is shown. (**i**) Rat pHS cells treated with VA-lip-siRNAgp46 or with VA-lip-siRNArandom and collagen deposition on tissue culture plates were assayed 1 d after transfection by the dye-binding method. Data were expressed as mean ± s.d., calculated from five transfections and as a percentage of untreated control. *$P < 0.01$ versus VA-lip-siRNAgp46. NS, not significant.

Optimal ratio of vitamin A to liposome

To determine the optimal vitamin A/liposome ratio for transduction of siRNAgp46 into HS cells, we incubated liposomes carrying siRNAgp46 coupled to carboxyfluorescein (FAM) (lip-siRNAgp46-FAM) with vitamin A in fractionated molar ratios ranging from 1:2 to 16:1. After removing free vitamin A by ultrafiltration, transduction efficiency by the vitamin A–bound lip-siRNAgp46-FAM (VA-lip-siRNAgp46-FAM) of rat primary HS cells (pHS cells) was examined using fluorescence-associated cell sorting (FACS). The highest mean fluorescence intensity (MFI) levels were observed at a molar vitamin A/liposome ratio of 2:1 in the incubation solution (**Supplementary Fig. 2** online). We used complexes at this incubation molar ratio, which corresponded to 0.65 mol vitamin A per mol cationic lipid in liposomes, in all subsequent experiments.

Confirmation of RBP binding to VA-lip-siRNAgp46

We used gel filtration to separate VA-lip-siRNAgp46 and vitamin A–free lip-siRNAgp46, both of which had been incubated with RBP. RBP from the VA-lip-siRNAgp46 preparation eluted with liposomes in the void volume. In contrast, RBP from lip-siRNAgp46 preparations eluted after the void volume, in fractions not containing liposomes (**Supplementary Fig. 3** online). This confirms binding of RBP to VA-lip-siRNAgp46.

Sizes of vitamin A–coupled liposomes

We used dynamic light scattering to compare the average sizes of vitamin A–coupled liposome, lip-siRNAgp46, VA-lip-siRNAgp46 and RBP-bound VA-lip-siRNAgp46 preparations with those of unmodified liposomes. From largest to smallest, particle sizes were: liposome, vitamin A–coupled liposome, lip-siRNAgp46, VA-lip-siRNAgp46 and RBP-bound VA-lip-siRNAgp46 (**Supplementary Table 1** online).

Receptor-mediated uptake of VA-lip-siRNAgp46-FAM by pHS cells

To verify the specific uptake of vitamin A–coupled liposomes by HS cells via the RBP receptor, we incubated rat pHS cells with VA-lip-siRNAgp46-FAM in the presence of various concentrations (0.07 μg/ml–1.4 μg/ml) of RBP and examined FACS patterns of the cells. Because the nonspecific lipofection rate increased and became more similar to that of receptor-mediated transduction with longer transduction times (data not shown), transduction time was limited to 30 min to distinguish between receptor-mediated transduction efficacy of VA-lip-siRNAgp46 and nonspecific transduction efficacy of lip-siRNAgp46. Rat pHS cells treated with VA-lip-siRNAgp46-FAM showed increasing fluorescence intensities as RBP concentrations increased from 0.07 μg/ml to 0.7 μg/ml, and the intensity plateaued at concentrations >0.7 μg/ml RBP (**Fig. 1e**). To further confirm specific uptake of vitamin A–coupled liposome/RBP complex by RBP receptors, we added anti-RBP antibody to the incubation medium of rat pHS cells treated with VA-lip-siRNAgp46-FAM in the presence of RBP (0.7 μg/ml). The MFI of these cells was suppressed by anti-RBP antibody, to levels near those with lip-siRNAgp46-FAM (**Fig. 1e**). Preferential uptake of VA-lip-siRNAgp46-FAM relative to that of lip-siRNAgp46-FAM was not observed using primary skin fibroblasts from normal rats (**Fig. 1f**). We conducted similar experiments to those involving pHS cells, using LI90 cells (an activated human HS cell line)[14] and found essentially the same results (**Fig. 1g**).

Intracellular transport of VA-lip-siRNAgp46-FAM in rat pHS cells

To elucidate the subcellular localization of siRNAgp46-FAM after uptake by RBP receptors, we monitored VA-lip-siRNAgp46-FAM–treated rat pHS cells and lip-siRNAgp46-FAM–treated rat pHS cells using fluorescence microscopy (**Fig. 1h**). In cells treated with VA-lip-siRNAgp46-FAM, fluorescence appeared as a faint granular pattern in the cytoplasm at 30 min, and as a denser granular pattern in the perinuclear region at 2 h. In contrast, no green fluorescence was seen in the cytoplasm of cells treated with lip-siRNAgp46-FAM after 30 min. Moreover, perinuclear fluorescence at 2 h was very faint.

VA-lip-siRNAgp46 suppresses collagen secretion of pHS cells

To validate the effect of VA-lip-siRNAgp46 on collagen secretion from rat pHS cells, we assessed the amount of collagen deposited on tissue culture plates by Sirius red dye binding and spectrophotometry and found it to be significantly lower than in untreated and VA-lip-siRNArandom-treated cells ($P < 0.01$) (**Fig. 1i**).

Delivery of VA-lip-siRNAgp46-FAM to HS cells in cirrhotic rat liver

Receptor-mediated uptake of vitamin A–coupled liposomes by HS cells *in vivo* was verified in rats previously treated with DMN (12 intraperitoneal injections over 4 weeks; **Supplementary Fig. 4** online) and then injected with VA-lip-siRNAgp46-FAM (3 injections, each 0.75 mg/kg siRNA and given every other day). The tissue distribution of siRNAgp46-FAM was examined by fluorescent emission 24 h after the final injection. Fluorescence of siRNAgp46-FAM (green) was identified in liver, predominantly in the region that stained positive for α-smooth muscle actin (α-SMA, red; an indicator of activated HS cells) giving rise to areas with a merged yellow color. The yellow area in ten randomly selected high-power (×630) fields from each specimen occupied 61.2 ± 9.8% of the area stained for α-SMA (**Fig. 2a**, images i,v). By contrast, the yellow area in α-SMA–positive regions (**Fig. 2a**, image iii) was negligible (5.6 ± 2.3%) in a rat injected with lip-siRNAgp46-FAM.

To confirm the specific delivery of siRNAgp46 to HS cells *in vivo*, we performed FACS analyses of cyanine 5 (Cy5) fluorescence intensity in hepatocytes, HS cells and Kupffer cells isolated from the liver of DMN-treated rats injected with VA-lip-siRNAgp46-Cy5. We observed markedly greater accumulation of siRNAgp46-Cy5 in α-SMA–positive cells (HS cells) than in CD 163–positive cells (Kupffer cells) or albumin-positive cells (hepatocytes). Accumulation of siRNAgp46-Cy5 in HS cells was not evident in rats injected with lip-siRNAgp46-Cy5 (**Fig. 2b**).

In the lung of a rat injected with VA-lip-siRNAgp46-FAM, very few cells, other than endothelial cells (alveolar epithelium) that showed autofluorescence, were positive for fluorescent emission and the fluorescence (green) of these cells merged with the red-staining of macrophages (CD68) indicating nonspecific uptake of siRNAgp46-FAM by macrophages. Similarly, fluorescent cells in the spleen of the same rat merged with red-stained macrophages, generating a yellow signal. Analyses of lungs and spleens from rats injected with lip-siRNAgp46-FAM showed results similar to those with VA-lip-siRNAgp46-FAM (**Fig. 2c**), indicating that nonspecific uptake of siRNAgp46-FAM by macrophages also occurred in both organs. The retina, which requires vitamin A for its photoreceptor function, showed almost no staining in either of the treated rats (**Fig. 2c**).

To further elucidate the pharmacodynamics and tissue distribution of VA-lip-siRNAgp46, radiolabeled liposomes carrying siRNAgp46 with [^{3}H]vitamin A were injected, through the tail vein, into normal rats and rats 24 d after commencement of the induction of acute cirrhosis by DMN (day 24 rats; **Fig. 2d**). The circulating half-lives of [^{3}H]VA-lip-siRNAgp46 were 19 min and 61 min for DMN-treated rats and normal rats, respectively, compared with 13 min for [^{3}H]vitamin A (**Fig. 2d**, insert) in cirrhotic rats. Radioactivity was found almost exclusively in cirrhotic livers 24 h after injection (**Fig. 2d**). An equal dose of radiolabeled vitamin A–coupled liposomes carrying

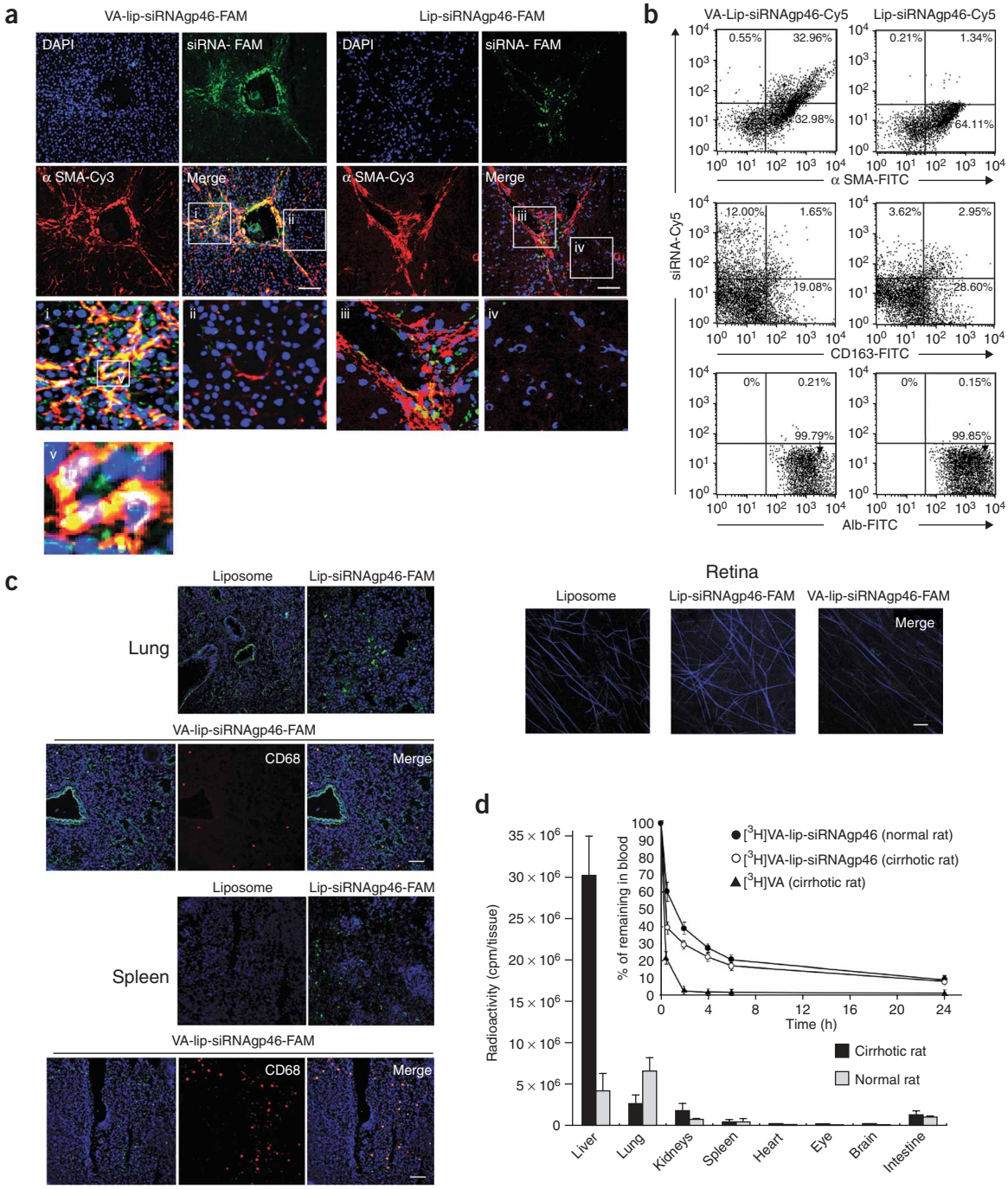

Figure 2 Specific delivery of VA-lip-siRNAgp46 to HS cells in cirrhotic rats. (**a**) Representative fluorescent images of α-SMA visualized by Cy3-conjugated anti-α-SMA antibody (red), nuclei counterstained with DAPI (blue) and siRNAgp46-FAM (green) in liver specimens from DMN-treated cirrhotic rats (day 24 rat) injected with VA-lip-siRNAgp46-FAM or lip-siRNAgp46-FAM every other day (three injections in total). The liver specimens were harvested 24 h after the last injection. Pictures taken at original magnification (×200) and magnified images corresponding to the areas enclosed in boxes are presented in i, ii and iii, iv. Image v: a high power image of i showing fluorescent staining in the cytoplasm. Scale bars, 100 μm. (**b**) Rat HS cells, Kupffer cells and hepatocytes rich fractions harvested 24 h after three injections of VA-lip-siRNAgp46-Cy5 or lip-siRNAgp46-Cy5 were stained with anti α-SMA-FITC, anti-rat CD168-FITC and anti-albumin-FITC (alb-FITC), respectively, and were analyzed by flow cytometry. (**c**) Representative immunofluorescent staining of macrophages with the Alexa 568-labeled anti-CD68 antibody (red) and siRNAgp46-FAM (green) in the lung, spleen and retina. Histologic sections from these organs were collected 24 h after i.v. injection of VA-lip-siRNAgp46-FAM, lip-siRNAgp46-FAM or liposomes. Fluorescent images of these sections were obtained using a confocal laser microscope. Scale bars, 100 μm. (**a–c**) Similar results were obtained in five independent experiments. (**d**) Representative tissue biodistribution and pharmacokinetics of [^{3}H]VA-lip-siRNAgp46 in rats. DMN-treated cirrhotic rats (day 24 rat) or normal rats ($n = 3$ per group) received a single i.v. injection of 200 μCi [^{3}H]VA-lip-siRNAgp46 via the tail vein. Tissue biodistribution was analyzed 24 h later. Data represent means ± s.d. ($n = 3$). The inserted figure shows the percentage of the injected dose remaining in the blood at the indicated times after infection. Each point represents the mean ± s.d. ($n = 3$). Similar results were obtained in two independent experiments.

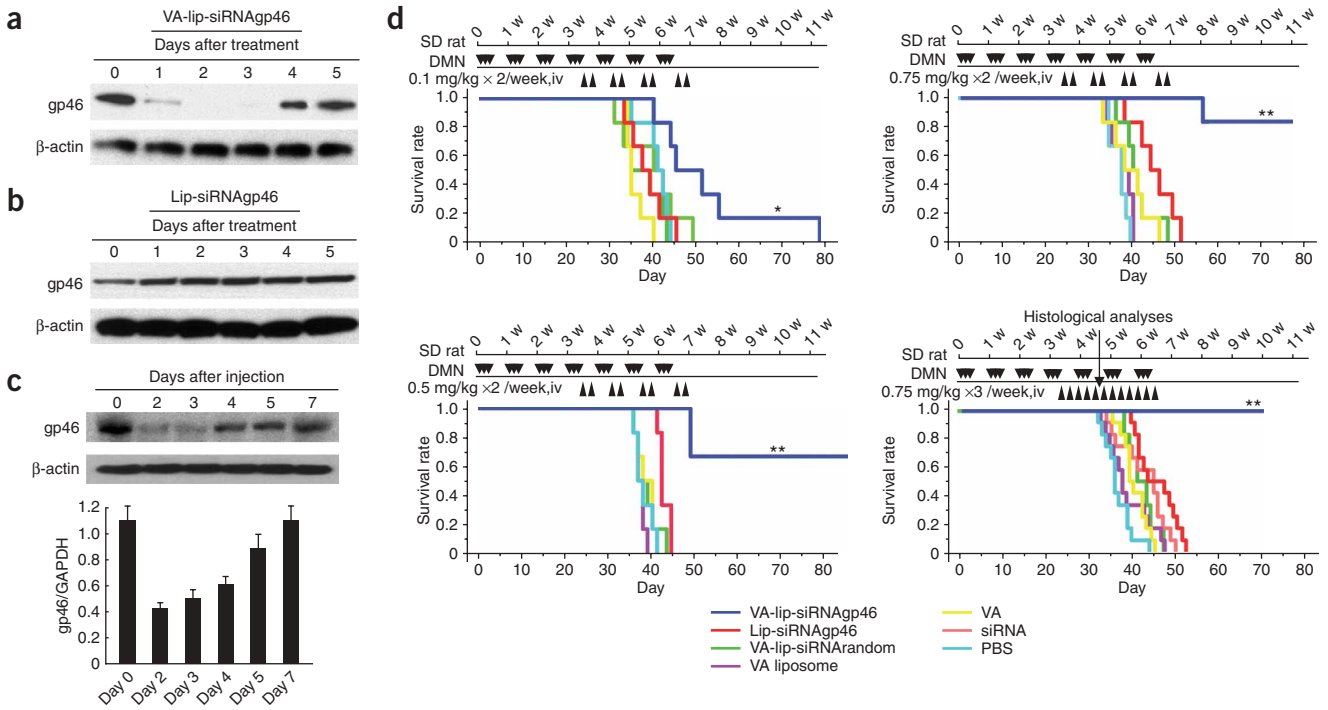

Figure 3 Effect of i.v. injected VA-lip-siRNAgp46 on cirrhotic rat survival. (**a**,**b**) Duration of suppressive effect of siRNAgp46 on gp46 expression in HS cells. Rat pHS cells were treated with VA-lip-siRNAgp46 (**a**) or lip-siRNAgp46 (**b**). At 30 min, the medium was replaced with fresh medium. At the time indicated, the expression of gp46 and β-actin (normalization control) were analyzed by western blotting. Similar results were obtained in three independent experiments. (**c**) The time course of gp46 expression in DMN-cirrhotic rats treated with VA-lip-siRNAgp46 (siRNA 0.75 mg/kg, one injection at day 24, $n = 3$). At the indicated time, western blot analysis (top) and quantitative real-time PCR (bottom) were used to analyze the expression of gp46. Liver gp46 mRNA levels were quantified relative to GAPDH mRNA. Data are mean ± s.d. from an analysis representative of three rats. (**d**) Survival of DMN-treated rats that were injected intravenously with VA-lip-siRNAgp46 at siRNA doses of 0.1, 0.5 or 0.75 mg/kg twice a week ($n = 6$ per group), or 0.75 mg/kg 3 times a week ($n = 12$ per group). In the control groups, DMN-treated rats were injected with lip-siRNAgp46, VA-lip-siRNArandom, vitamin A–coupled liposomes, vitamin A, PBS ($n = 6$ for each group of 0.1, 0.5 or 0.75 mg/kg twice a week, $n = 12$ for each group of 0.75 mg/kg 3 times a week) or siRNAgp46 ($n = 12$ for group of 0.75 mg/kg siRNA, three times a week). Life-table analyses are presented as a Kaplan-Meyer plot. (*$P < 0.05$; **$P < 0.0001$ compared with control rats).

siRNAgp46 injected into a noncirrhotic rat of equal age substantially reduced accumulation of radioactivity in all organs. This indicates that HS cells, which specifically took up VA-lip-siRNAgp46, had not proliferated to the same extent in normal livers as in cirrhotic livers.

Duration of gp46 suppression by VA-lip-siRNAgp46

To examine the duration of the effect of siRNAgp46 on gp46 expression, we treated rat pHS cells with VA-lip-siRNAgp46 and lip-siRNAgp46 *in vitro* for 30 min (**Fig. 3a**,**b**) and intravenously injected VA-lip-siRNAgp46 in DMN rats at day 24 (**Fig. 3c**). Both the rat pHS cells and the livers of DMN rats showed suppressed gp46 expression for at least 3 d (**Fig. 3a**,**c**) whereas treatment of pHS cells with lip-siRNAgp46 did not suppress gp46 expression (**Fig. 3b**).

Survival of DMN rats by i.v. treatment with VA-lip-siRNAgp46

We examined the effect of siRNAgp46 on survival of rats exposed to normally lethal DMN treatments[6] (**Fig. 3d**). In this series of experiments, treatments were begun after induction of liver cirrhosis (day 24) by 12 administrations of DMN (**Supplementary Fig. 4**). Controls treated with PBS, vitamin A, vitamin A–coupled liposome, VA-lip-siRNArandom or lip-siRNAgp46 twice weekly all died within 52 d after DMN treatment.

DMN-treated rats appeared to die from hepatic failure because they developed ascites, gastrointestinal bleeding and tarry feces (data not shown). In contrast, rats treated with VA-lip-siRNAgp46 twice weekly showed a dose-dependent (0.1, 0.5, 0.75 mg/kg) prolongation of survival time and a much higher survival rate (83.3%; 5/6 rats) at 0.75 mg/kg. Survival was 100% (12/12) when the 0.75 mg/kg dose was given three times per week (**Fig. 3d**)—a finding compatible with the observation that gp46 expression was suppressed for 72 h but restored within 4 d after siRNAgp46 treatment (**Fig. 3a**,**c**).

Resolution of hepatic fibrosis by siRNAgp46 in DMN-treated rats

Liver fibrosis in DMN-treated rats (day 33) that received VA-lip-siRNAgp46 (0.75 mg/kg) five times was examined using Azan-Mallory (**Fig. 4a**) and collagen I staining (**Fig. 4b**). The fibrotic area detected by computerized image analysis scoring for collagen staining was significantly smaller in specimens from VA-lip-siRNAgp46–treated rats than in control specimens ($P < 0.001$) (**Fig. 4c**); these results were consistent with quantitative RT-PCR data for procollagen type I and TIMP-1 mRNA, which showed substantial suppression of mRNA expression by VA-lip-siRNAgp46 treatment (**Fig. 4d**). Similarly, hydroxyproline levels in VA-lip-siRNAgp46–treated rats were significantly lower than in control rats ($P < 0.001$) (**Fig. 4e**). Pathological staging, that is, fibrosis and architectural alteration, was also clearly suppressed in VA-lip-siRNAgp46–treated rats (**Fig. 4f**).

The effect of siRNAgp46 on hepatic gp46 expression was also examined by staining for gp46 in liver specimens of rats injected

with VA-lip-siRNAgp46 and VA-lip-siRNArandom five times (day 33). The positively stained area (red) was substantially smaller in the former (**Fig. 4g**). Western blot analysis results were compatible with this immunohistological observation; the intensity of the gp46 band was weaker in VA-lip-siRNAgp46–treated rats than in controls (**Fig. 4h**).

The reversibility of liver cirrhosis was examined in liver specimens from day 47 and day 70 rats that stopped receiving DMN and VA-lip-siRNAgp46 treatments at day 44 and day 46, respectively. Near-complete restoration of normal hepatic architecture was observed in specimens from day 47 and day 70 rats (**Fig. 4i**), indicating the regeneration capacity of liver tissue.

Induction of apoptosis in rat HS cells by siRNAgp46

This observation led us to speculate that siRNAgp46 treatment might induce apoptotic death of HS cells. Apoptosis was determined by TUNEL staining on day 33 liver specimens from DMN-treated rats injected with VA-lip-siRNAgp46 (0.75 mg/kg five times on every other day), PBS, vitamin A alone, vitamin A–coupled liposomes, VA-lip-siRNArandom or lip-siRNAgp46; ($n = 3$ per group). TUNEL-positive cells in areas overlapping with HS cells (α-SMA positive) apparently increased in rats treated with VA-lip-siRNAgp46 versus VA-lip-siRNArandom (**Supplementary Fig. 5a** online). TUNEL-positive cells in α-SMA–positive areas (**Supplementary Fig. 5b**) significantly increased in VA-lip-siRNAgp46–treated rats relative to controls ($P < 0.01$).

In HS cell–cultivation experiments, TUNEL staining in apoptotic nuclei of rat pHS cells transfected by siRNAgp46 was greater after 3 d than in control HS cells (**Supplementary Fig. 5c**). Approximately half (48 ± 12%) of all nuclei in siRNAgp46-transfected HS cells were apoptotic—a substantial increase relative to controls ($P < 0.01$) (**Supplementary Fig. 5d**). These results suggest that siRNAgp46 not only inhibits secretion of collagen from HS cells but also abrogates HS cells in fibrotic tissue through apoptosis, culminating in the blockage of further collagen accumulation in the tissue.

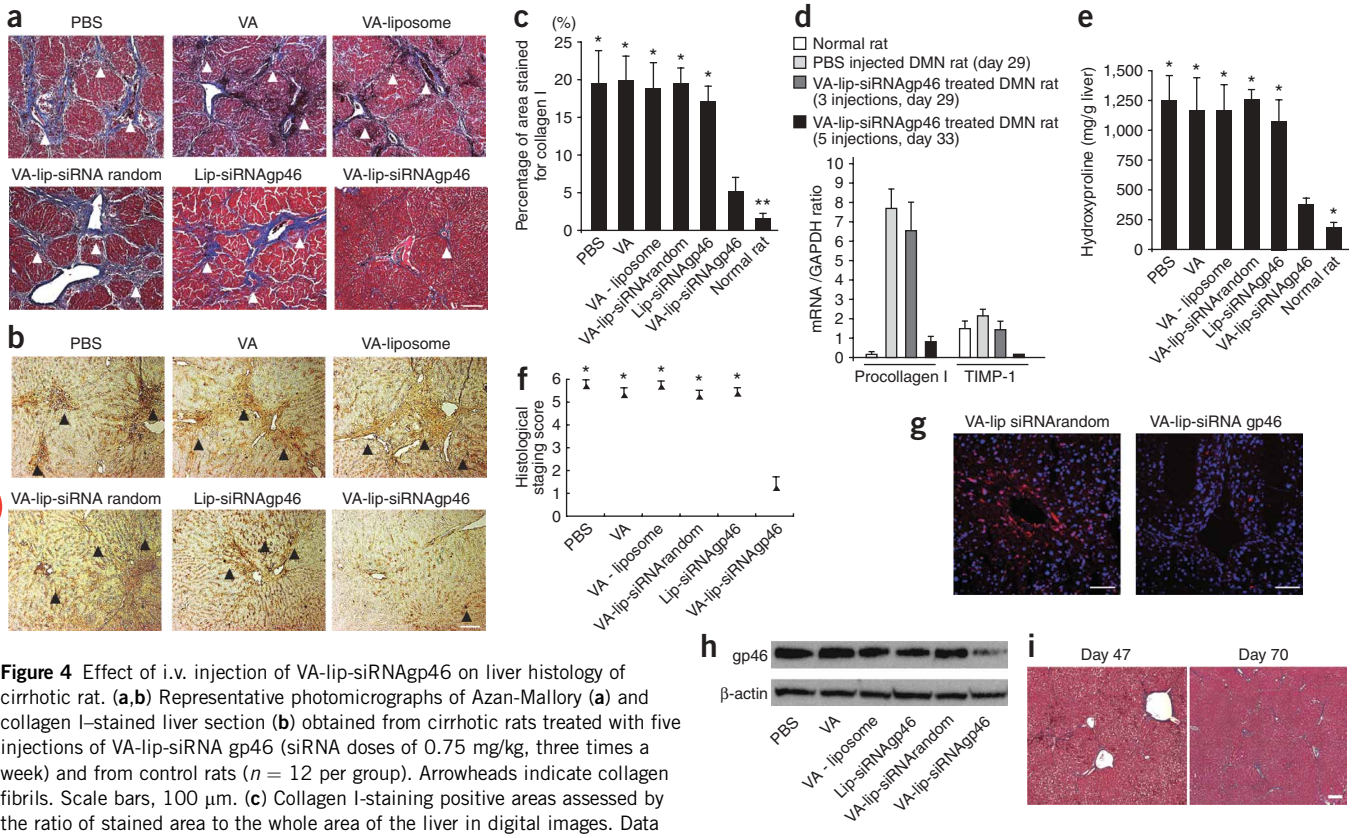

Figure 4 Effect of i.v. injection of VA-lip-siRNAgp46 on liver histology of cirrhotic rat. (**a**,**b**) Representative photomicrographs of Azan-Mallory (**a**) and collagen I–stained liver section (**b**) obtained from cirrhotic rats treated with five injections of VA-lip-siRNA gp46 (siRNA doses of 0.75 mg/kg, three times a week) and from control rats ($n = 12$ per group). Arrowheads indicate collagen fibrils. Scale bars, 100 μm. (**c**) Collagen I-staining positive areas assessed by the ratio of stained area to the whole area of the liver in digital images. Data were obtained from six randomly selected fields in each 12-rat group and represent the mean ± s.d. $^*P < 0.001$; $^{**}P < 0.01$ versus VA-lip-siRNAgp46. (**d**) The expression of procollagen I and TIMP-1 mRNA in normal rats ($n = 3$), DMN-treated cirrhotic rats treated with three injections of PBS ($n = 3$), DMN-cirrhotic rats treated with three injections of VA-lip-siRNAgp46 ($n = 3$), and DMN-cirrhotic rats treated with five injections of VA-lip-siRNAgp46 ($n = 3$) were quantified by real-time PCR. Expression was normalized as the ratio to GAPDH mRNA, a housekeeping gene. Data are mean ± s.d. from one analysis representative of three different rats. (**e**) Hydroxyproline content in the livers. Mean ± s.d. of 12 rats per group. $^*P < 0.001$ versus VA-lip-siRNAgp46. (**f**) Semiquantitative scoring analysis for histological staging. Liver tissues were obtained from rats treated as described in **a**. Values are means ± s.d. ($n = 12$ per group). $^*P < 0.001$ versus VA-lip-siRNAgp46. (**g**) Representative immunofluorescent staining patterns for gp46 in cirrhotic liver of rats (day 24 rat) injected with VA-lip-siRNArandom ($n = 3$) or VA-lip-siRNAgp46 ($n = 3$) three times every other day obtaining 24 h after the last injection. Immunofluorescent images of gp46 stained with Alexa 568-labeled anti-gp46 antibody (red) and of nuclei counterstained with DAPI (blue) were obtained using a confocal laser microscope. Scale bars, 100 μm. Western blot analysis of gp46 in the liver homogenates (**h**) showed essentially the same results as the histological analyses; that is, suppression of the gp46 band by VA-lip-siRNAgp46 treatment. Results from each group of three rats were essentially similar. (**i**) Representative Azan-Mallory-stained liver section from day 47 and day 70 rats. Results from each group of six rats were essentially similar. Scale bars, 200 μm.

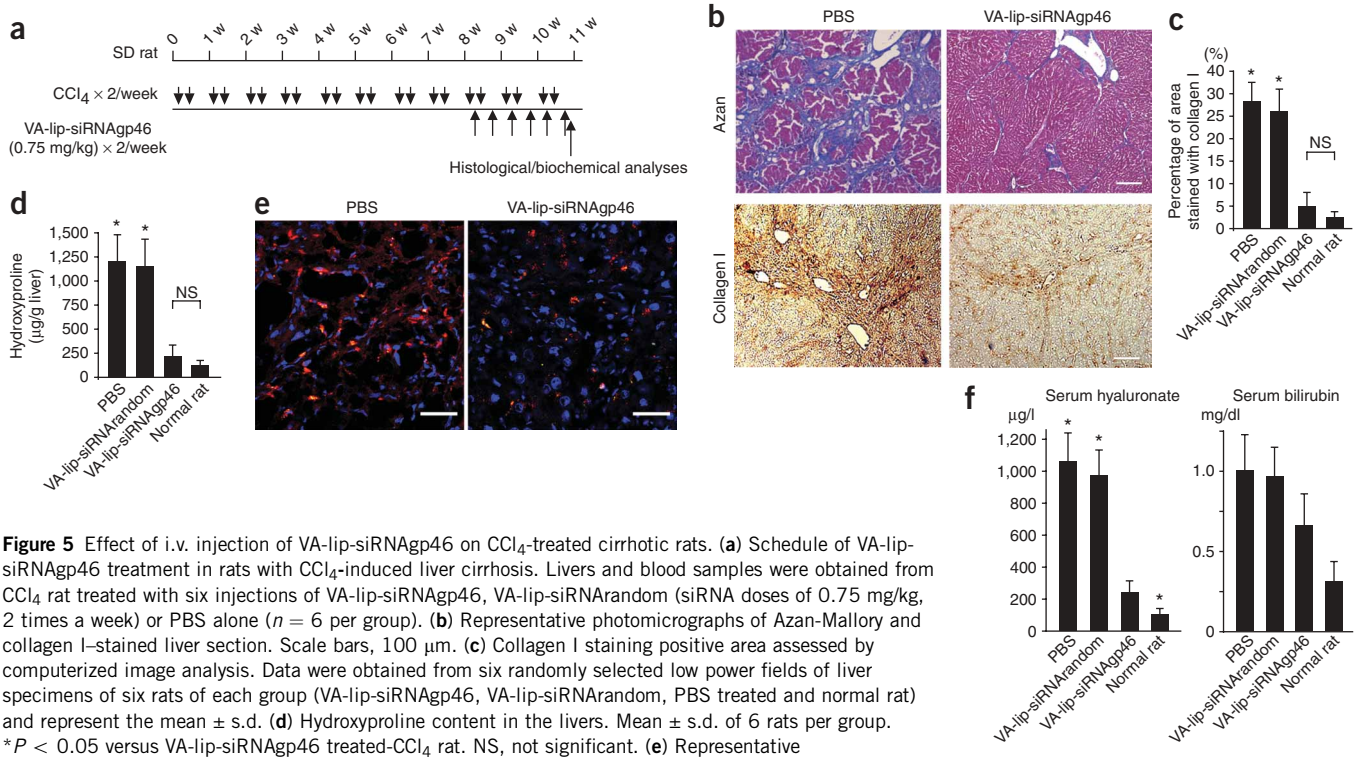

Figure 5 Effect of i.v. injection of VA-lip-siRNAgp46 on CCl_4-treated cirrhotic rats. (**a**) Schedule of VA-lip-siRNAgp46 treatment in rats with CCl_4-induced liver cirrhosis. Livers and blood samples were obtained from CCl_4 rat treated with six injections of VA-lip-siRNAgp46, VA-lip-siRNArandom (siRNA doses of 0.75 mg/kg, 2 times a week) or PBS alone ($n = 6$ per group). (**b**) Representative photomicrographs of Azan-Mallory and collagen I–stained liver section. Scale bars, 100 μm. (**c**) Collagen I staining positive area assessed by computerized image analysis. Data were obtained from six randomly selected low power fields of liver specimens of six rats of each group (VA-lip-siRNAgp46, VA-lip-siRNArandom, PBS treated and normal rat) and represent the mean ± s.d. (**d**) Hydroxyproline content in the livers. Mean ± s.d. of 6 rats per group. $^*P < 0.05$ versus VA-lip-siRNAgp46 treated-CCl_4 rat. NS, not significant. (**e**) Representative immunofluorescent images of gp46 stained with Alexa 568-labeled anti-gp46 antibody (red) and of nuclei counterstained with DAPI (blue) were obtained using a confocal laser microscope. Scale bars, 100 μm. Results from each group of three rats were essentially similar. (**f**) Total bilirubin and hyaluronate levels in the sera of rats. Values are the mean ± s.d. for each group ($n = 6$ per group). $^*P < 0.05$ versus VA-lip-siRNAgp46 treated-CCl_4 rats.

Effects of siRNAgp46 treatment on liver function

VA-lip-siRNAgp46 (0.75 mg/kg, five times on every other day) significantly attenuated the elevation of serum bilirubin and hyaluronate in VA-lip-siRNAgp46–treated cirrhotic rats relative to control cirrhotic rats at day 33, during DMN exposure ($P < 0.01$). At day 70, bilirubin, hyaluronate, alanine aminotransferase (ALT) and albumin levels in DMN rats were nearly or completely normalized by VA-lip-siRNAgp46 treatment (**Supplementary Fig. 6** online).

Effects of siRNAgp46B and siRNAgp46C on DMN cirrhosis

To eliminate the possibility that the *in vitro* and *in vivo* results obtained by treatment with siRNAgp46A resulted from off-targeting effects, we tested the effect of the two other siRNAs for gp46, siRNAgp46B and C, on cirrhosis in DMN-treated rats. Prolonged survival, reduced histological fibrosis and suppression of hydroxyproline accumulation were clearly associated with exposure to either siRNA (**Supplementary Fig. 7** online), indicating that the effects of siRNAgp46A were not related to off-targeting.

VA-lip-siRNAgp46 does not trigger immune reaction

Interferon-α (IFN-α) mRNA expression in the liver, spleen and lung remained normal after VA-lip-siRNAgp46 treatment (**Supplementary Table 2** online). As siRNAβgal728 complexed to lipofectamine-2000 reportedly induces immune reactions in mammals[15] (**Supplementary Methods** online), we also tested the serum concentrations of TNF-α and IL-12 in rats treated with VA-lip-siRNAgp46 or siRNAβgal728 complexed to lipofectamine-2000. Serum concentrations of TNF-α and IL-12 remained normal after VA-lip-siRNAgp46 treatment, in contrast to the significantly elevated values in rats treated with siRNAβgal728 complexed to lipofectamine-2000 ($P < 0.05$) (**Supplementary Table 2**).

Collagenase activity in liver of siRNAgp46-treated cirrhotic rats

To assess collagenolytic activity in the cirrhotic liver, we measured collagenase activity in liver homogenates from DMN rats. Collagenase activity in DMN-treated rats injected with PBS or VA-lip-siRNAgp46 three times (day 29) was as high as in normal liver and remained high after five treatments with VA-lip-siRNAgp46 (day 33) (**Supplementary Table 3** and **Supplementary Methods**).

Effect of VA-lip-siRNAgp46 on CCl_4-induced cirrhosis

Serial intraperitoneal treatment of rats with CCl_4 (16 times over 8 weeks) causes nonlethal liver cirrhosis[4]. We used this additional model of chemically induced cirrhosis to further assess the antifibrotic potential of siRNAgp46 and VA-lip-siRNAgp46 by administering them twice weekly for 3 weeks (**Fig. 5a**). The effect of siRNAgp46 was essentially the same as in DMN-treated rats with respect to shrinkage of the fibrotic area (**Fig. 5b,c**), suppression of hydroxyproline levels (**Fig. 5d**) and gp46 expression (**Fig. 5e**). Bilirubin and hyaluronate levels were also improved in CCl_4-treated cirrhotic rats treated with VA-lip-siRNAgp46 (**Fig. 5f**).

Effect of VA-lip-siRNAgp46 on bile duct ligation–induced cirrhosis

To verify that our modality is also effective for cirrhosis induced by chronic continuous stimulation with bile regurgitation, we administered VA-lip-siRNAgp46 to rats that underwent bile duct ligation[16] (BDL; **Fig. 6a**). Histological improvement of fibrosis (**Fig. 6b,c**) and suppression of hydroxyproline levels (**Fig. 6d**), serum bilirubin and hyaluronate levels (**Fig. 6e**) were clearly observed at day 45 after five injections of VA-lip-siRNAgp46 (0.75 mg/kg, every other day). These effects were maintained until day 67 by consecutive injection of the same agents twice a week (**Fig. 6f–i**), although BDL stimulation

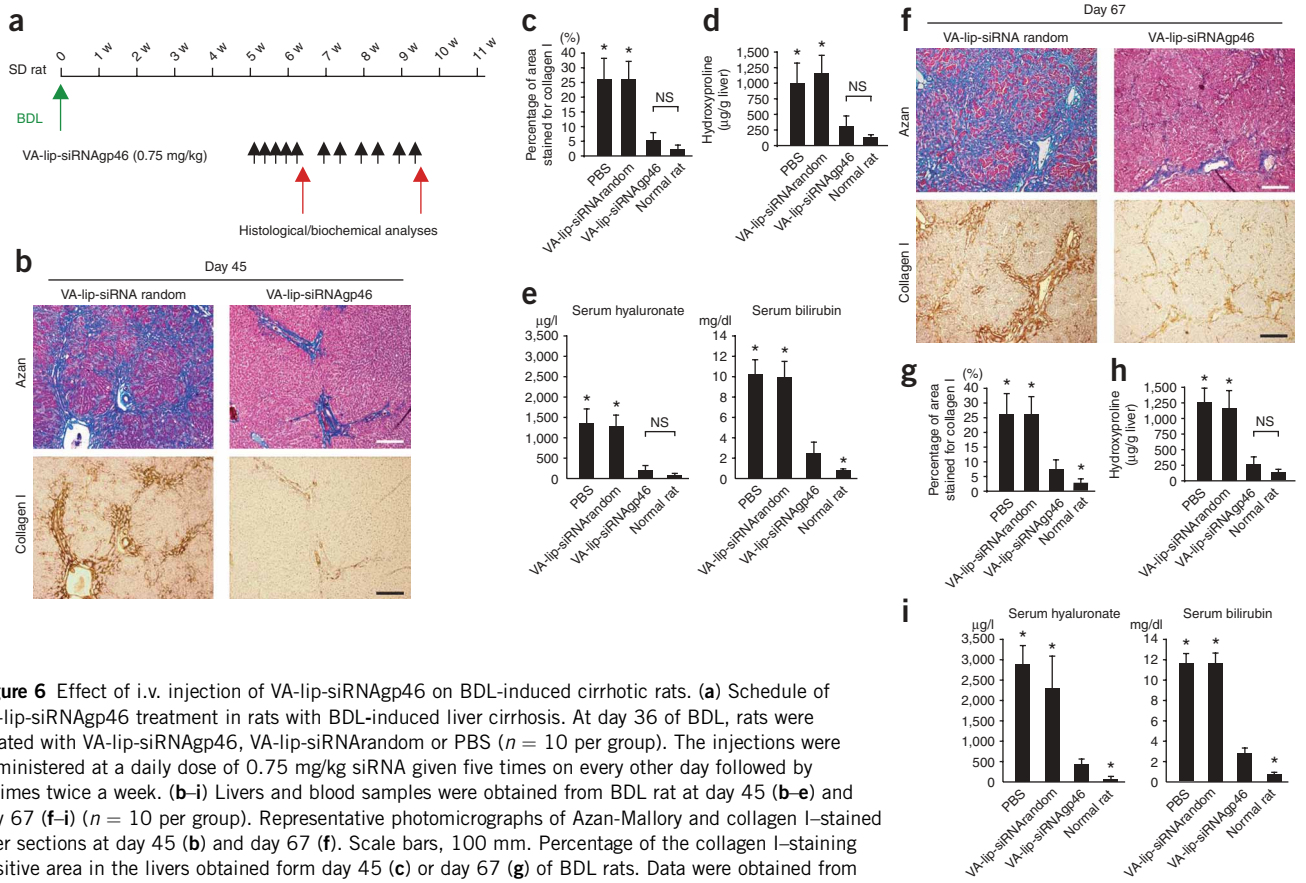

Figure 6 Effect of i.v. injection of VA-lip-siRNAgp46 on BDL-induced cirrhotic rats. (**a**) Schedule of VA-lip-siRNAgp46 treatment in rats with BDL-induced liver cirrhosis. At day 36 of BDL, rats were treated with VA-lip-siRNAgp46, VA-lip-siRNArandom or PBS ($n = 10$ per group). The injections were administered at a daily dose of 0.75 mg/kg siRNA given five times on every other day followed by 6 times twice a week. (**b**–**i**) Livers and blood samples were obtained from BDL rat at day 45 (**b**–**e**) and day 67 (**f**–**i**) ($n = 10$ per group). Representative photomicrographs of Azan-Mallory and collagen I–stained liver sections at day 45 (**b**) and day 67 (**f**). Scale bars, 100 mm. Percentage of the collagen I–staining positive area in the livers obtained form day 45 (**c**) or day 67 (**g**) of BDL rats. Data were obtained from six randomly selected low power fields of liver specimens of ten rats of each group (VA-lip-siRNAgp46, VA-lip-siRNArandom, PBS treated and normal rat) and represent the mean ± s.d. Hydroxyproline content in the livers obtained form day 45 (**d**) or day 67 (**h**) of BDL rats. Data were obtained from ten rats in each group and represent the mean ± s.d. Total bilirubin and hyaluonate levels in the sera of rats obtained form day45 (**e**) or day 67 (**i**). Values are the mean ± s.d. for each group ($n = 10$ per group). $^*P < 0.05$ versus VA-lip-siRNAgp46-treated-BDL rat.

persisted as evidenced by marked bile duct proliferation accompanied by fibrosis in PBS- or VA-lip-siRNArandom–treated groups.

DISCUSSION

The inadequate target specificity of most approaches to treat liver fibrosis has limited their suitability for clinical use[17]. Our two-pronged strategy to ensure specificity involves, first, targeting a collagen-specific chaperone molecule (gp46) with siRNA and, second, delivery of siRNA specifically to collagen-producing liver cells, using vitamin A–coupled liposomes. This enabled us to resolve hepatic collagen deposition in rat models involving induction of cirrhosis by either DMN or CCl_4 treatments or bile duct ligation. Survival of DMN-treated rats was prolonged in a dose-and duration-dependent manner, indicating a biologically specific effect of siRNAgp46 treatment.

Off-target effects[18] and immune responses, such as induction of interferon (IFN-α) driven by the interaction with Toll-like receptor (TLR)3 or TLR 7/8 (ref. 15), are two issues often associated with the use of siRNA that can lead to misinterpretation of siRNA experiments. We used three independent siRNAs against the same target (gp46) mRNA and found comparable gene silencing efficacy and antifibrotic effects *in vivo* (**Fig. 1a** and **Supplementary Fig. 7**), suggesting that the phenotype observed with downregulation of gp46 was indeed related to gp46 knockdown and not a bystander effect of the siRNA sequence. To circumvent immune responses such as induction of IFN-α, we used siRNA with a 2-nucleotide 3′ overhang, shown to impair activation of the transcription factor IRF3 (ref. 19). In addition, our siRNA did not contain the 5′ triphosphate of the T7-transcript (manufacturer's information), which reportedly plays a role in IFN induction[20]. In fact, there was no elevation of either IFN-α mRNA in the liver or TNF-α and IL-12 in the circulation of rats treated with VA-lip-siRNAgp46. However, as the modifications of siRNA described above may not prevent the triggering of all immune responses, it is possible that the low immune activation in the present investigation was relevant to the RBP receptor–mediated uptake of siRNA, in addition to the modifications of siRNA structure.

Although specificity is important, another critical factor in the use of siRNAs as therapeutic agents is the efficacy of suppression of the target molecule. As synthetic RNA duplexes 25–30 nucleotides in length are up to 100-fold more potent than corresponding conventional 21-mer siRNA[21], we used a 27-nucleotide RNA duplex with 2-nucleotide 3′ overhangs.

Another factor influencing the efficacy of siRNA treatment is the duration of gene silencing, which is mainly governed by dilution resulting from cell division. In rapidly dividing tumor cells, recovery of protein levels suppressed by siRNAs to pretreatment levels occurs within <1 week, whereas in slow-dividing fibroblasts or in nondividing hepatocytes, it takes >3 weeks[22]. We confirmed that levels of gp46

in HS cells treated with siRNA remained suppressed for at least 72 h *in vitro* and *in vivo* and used 48–72 h as the siRNA injection interval to demonstrate *in vivo* efficacy.

The *in vivo* siRNA dose used in our study (0.75 mg/kg per single injection) was less than doses previously shown to have *in vivo* therapeutic effects[23–25]. This may be related to the use of vitamin A–coupled liposomes to preferentially deliver siRNAgp46 to HS cells. It has long been debated whether transfer of retinol from plasma RBP/retinol complex to cellular RBP in HS cells is receptor driven or proceeds by passive diffusion[26]. Findings from most recent studies are consistent with receptor-driven uptake of retinol by HS cells[27–30], although coexistence of direct positioning into the hydrophobic part of cell membranes and receptor-mediated uptake has not been entirely ruled out[31].

Consistent with the receptor-based theory, specific uptake of vitamin A–coupled liposomes by HS cells after binding to plasma RBP was shown in *in vitro* studies assessing RBP concentration–dependence, the effect of RBP antibody (**Fig. 1e**,**f**), and subcellular localization (**Fig. 1h**). Notably, siRNA-FAM fluorescence in the cirrhotic liver of rats injected intravenously with vitamin A–coupled liposomes was mainly observed in areas with HS cells (identified by α-SMA staining) but not in parenchymal areas. Along with the finding that the area where FAM-florescence and HS cells were merged was markedly greater than in rats treated with vitamin A–free liposomes, this is also compatible with the notion that vitamin A–coupled liposomes are specifically taken up into HS cells by RBP receptors. The observation that liver fibrosis underwent regression and that survival time was significantly prolonged only in animals treated with vitamin A–coupled liposomes carrying siRNAgp46 further supports the vitamin A–receptor theory (Breslow-Gehan Wilcoxon test, $P < 0.0001$).

Incidentally, our results also confirm that activated HS cells, which become free of vitamin A deposition during the activation process[1], take up vitamin A as effectively as resting HS cells, which store vitamin A[32]. Both an activated HS cell line (LI90) and primary rat liver HS cells activated by *in vitro* cultivation[33] expressed markedly enhanced FAM fluorescence when they were incubated with vitamin A–coupled liposomes instead of vitamin A–free liposomes (**Fig. 1e**,**g**).

VA-lip-siRNAgp46-FAM distribution was negligible in retina, presumably because the eye is an isolated system with a strong blood-retinal barrier[34]. It was slightly evident in spleen and liver, which showed uptake of VA-lip-siRNAgp46 in a vitamin A receptor–independent manner to the reticuloendothelial system (macrophages), although these cells are not primarily collagen-producing cells and therefore should not be affected by nonspecific uptake of siRNAgp46.

When organ distribution of radiolabeled vitamin A–coupled liposomes was examined, prominent uptake of radioactivity was seen only in cirrhotic livers. The radioactivity in other organs was essentially the same in both DMN-treated and normal rats, which indicated that the delivery of vitamin A–coupled liposomes was indeed specific to HS cells possessing RBP receptors, and that delivery to other tissues occurred in a nonspecific manner, probably through nonspecific engulfment by macrophages.

It is also noteworthy that our vitamin A–coupled liposome system for the delivery of siRNA appeared to be quite efficient compared with previously reported methods using conventional liposomes. Our vitamin A–coupled liposomes produced biological effects at a dose of 0.75 mg/kg liposome, whereas in previous reports[23,24,35,36], doses of ~8–160 mg/kg were necessary. Furthermore, most other studies[37] used approximately a 1:10 ratio of solution to total blood volume (that is, 200 μl/2 ml blood in mice; 2,000 μl/20 ml blood volume in rats) to dissolve liposomes containing siRNA for a single bolus injection. However, we used only 200 μl per injection for 200-g rats (1:100 blood volume). This suggests that in our study hydrodynamic pressure did not contribute to *in vivo* transduction of siRNA, whereas in previous studies, siRNAs might have been forcibly transduced by hydrodynamic pressure, at least to some extent. This may explain why background fluorescence for FAM was weak and showed low nonspecific distribution of radioactive vitamin A–coupled liposomes to tissues other than the liver.

Various animal models of liver fibrosis have been explored[4,6,16,38,39]. We chose to focus primarily on the DMN model because it causes progressive and lethal fibrosis, which enabled us to demonstrate prolonged survival resolution of fibrosis. We confirmed these results using both the CCl_4 model, which is nonlethal and has milder features than the DMN model, and bile duct ligation models, which induces chronic cirrhosis by continuous stimulation of bile regurgitation. The consistency of the findings across all three models indicates the applicability of our approach for various types of liver cirrhosis.

In these models, regression of fibrosis occurred after five injections of siRNAgp46, whereas the animals were still being exposed to DMN, CCl_4 or BDL stimulation. The primary mechanism underlying the therapeutic effect was surmised to be the inhibition of collagen secretion by siRNAgp46 (**Fig. 1c**,**d**,**i**) and concomitant degradation of predeposited collagen by collagenase activity, which remained as high as in normal liver until fibrosis was almost completely resolved by the five treatments with VA-lip-siRNAgp46 (**Supplementary Table 3**). This finding was consistent with the notion that matrix metalloproteinases, once they are secreted from cells, form a persistent extracellular matrix–associated pool by binding to type 1 collagen[40,41]. In addition, HS cell apoptosis, possibly resulting from loss of anchorage sites (collagen) is considered to be a secondary mechanism for the therapeutic effect (**Supplementary Fig. 5**). Incidentally, apparent suppression of procollagen I mRNA in siRNAgp46-treated liver (**Fig. 4d**), which should not be caused by siRNAgp46 *per se*, may also be ascribed to the apoptosis of collagen-producing HS cells.

The improvement of serum bilirubin and hyaluronate levels in all three cirrhosis models further substantiates resolution of fibrosis in the portal area. Serum albumin and ALT levels, however, were not significantly improved by VA-lip-siRNAgp46 treatment in DMN-treated rats. This may result from the toxic effect of ongoing DMN treatment, as DMN-treated rats at day 70 showed restoration of normal hepatic architecture (**Fig. 4i**) and nearly complete normalization of serum albumin and ALT levels in addition to serum bilirubin and hyaluronate (**Supplementary Fig. 6**). Therefore, our modality actually reverses liver cirrhosis both histologically and functionally. This underscores its promise for clinical translation to treat liver cirrhosis.

METHODS

Cell lines. Normal rat kidney fibroblast (NRK) cells and LI90 cells (human HS cell line) were obtained from RIKEN cell bank (RIKEN Institute). The cells were maintained in Dulbecco's modified Eagle's medium (DMEM; Life Technologies, Inc.) supplemented with 10% (wt/vol) FBS, 1 mM sodium pyruvate and 4 mM L-glutamine at 37 °C in 5% CO_2.

Preparation of siRNAs. Three formulations of siRNA directed against gp46 (GenBank accession no. M69246), a rat homolog of human HSP47, were purchased from Hokkaido System Science. The sense and anti-sense strands of siRNAs were: gp46 (sequence A), beginning at nt 757, 5′-GU UCCACCAUAAGAUGGUAGACAACAG-3′(sense); 5′-P. GUUGUCUACC AUCUUAUGGUGGAACAU-3′ (antisense); gp46 (sequence B), beginning

at nt 1626, 5′-P. CCACAAGUUUUAUAUCCAAUCUAGCAG-3′ (sense), 5′-GCUAGAUUGGAUAUAAAACUUGUGGAU-3′ (antisense); gp46 (sequence C), beginning at nt 1909, 5′-CUAGAGCCAUUACAUUACAUUGACAAG-3′ (sense); 5′-UGUCAAUGUAAUGUAAUGGCUCUAGAU-3′ (antisense). siRNA-random, 5′-CGAUUCGCUAGACCGGCUUCAUUGCAG-3′(sense) and 5′-GCAAUGAAGCCGGUCUAGCGAAUCGAU-3′ (antisense).

For some experiments, gp46 siRNA (sequence A) with 6′-carboxyfluorescein (6-FAM) or cyanine 5 (Cy-5)-coupled to the 5′ end of the sense strand was used. All of these sequences were shown by BLAST search to not share sequence homology with any known rat mRNA. For IFN response experiments, siRNA targeting β-galactosidase bearing a motif eliciting interferon production (siRNAβgal728), obtained from Dharmacon, Inc., was used[15].

Transfection of siRNAs. siRNAs were introduced into NRK cells by the use of Lipotrust (Hokkaido System Science) according to the manufacturer's protocol.

Western blot analysis. Protein extracts of cells or liver specimens were resolved over 4/20 SDS-polyacrylamide gels, transferred onto nitrocellulose membranes, probed with antibodies against HSP47 (gp46) (Stressgen) or β-actin (Cell Signaling), then with peroxidase-coupled antibodies as the secondary antibody (Oncogene Research Product). Lastly, they were visualized with ECL (Amersham Life Science).

Assay for collagen synthesis. Collagen synthesis in NRK cells was assessed by proline incorporation assay[42]. Briefly, 1×10^5 NRK cells were seeded in 6-well plates with culture medium containing 10% FBS. After 24 h, the cells were transfected with 50 nM of siRNAgp46 using Lipotrust and incubated for 24 h. Thereafter, the medium was changed to OPTI-MEM containing [2,3-^{3}H]-l-L-proline (5 μCi/ml, NEN). After 24 h, two 200-μl aliquots of culture supernatant were removed from each well.

Samples of supernatant were used to quantify total newly synthesized [^{3}H]proline-labeled protein production. The amount of noncollagen proteins and collagenase-digestible protein was measured in the second aliquot using collagenase (*Clostridium histolyticum*, Sigma). The radioactivity was measured by scintillation counting. The amount of collagen present in each culture supernatant was determined by subtracting the counts per minute (c.p.m.) obtained from the aliquot used to measure noncollagen protein from the c.p.m. obtained from the aliquot used to measure total protein. Data are expressed as the percent of collagen produced relative to control cultures.

Preparation of VA-coupled liposomes carrying siRNAgp46. Cationic liposomes (Lipotrust) containing *O,O′*-ditetradecanoyl-*N*-(α-trimethylammonioacetyl) diethanolamine chloride (DC-6-14) (**Supplementary Fig. 2a**) as a cationic lipid[43], cholesterol and dioleoylphosphatidylethanolamine at a molar ratio of 4:3:3 (which has shown high transfection efficiency under serum-containing conditions for *in vitro* and *in vivo* gene delivery[43,44]) were purchased from Hokkaido System Science. The liposomes were manufactured using the freeze-dried empty liposomes method described previously[43] and prepared at a concentration of 1 mM (DC-16-4) by addition of double-distilled water (DDW) to the lyophilized lipid mixture under vortexing before use. To prepare VA-coupled liposomes, 200 nmol of vitamin A (retinol, Sigma) dissolved in DMSO was mixed with the liposome suspensions (100 nmol as DC-16-4) by vortexing in a 1.5 ml tube at 25 °C. To prepare VA-coupled liposomes carrying siRNAgp46 (VA-lip-siRNAgp46), a solution of siRNAgp46 (580 pmol/μl in DDW) was added to the retinol-coupled liposome solution with stirring at 25 °C. The ratio of siRNA to DC-16-4 was 1:11.5 (mol/mol) and the siRNA to liposome ratio (wt/wt) was 1:1. Any free vitamin A or siRNA that was not taken up by liposomes were separated from liposomal preparations using a micropartition system (VIVASPIN 2 concentrator 30,000 MWCO PES, VIVASCIENCE). The liposomal suspension was added to the filters and centrifuged at 1,500*g* for 5 min 3 times at 25 °C. Fractions were collected and the material trapped in the filter was reconstituted with PBS to achieve the desired dose for *in vitro* or *in vivo* use.

Isolation of rat HS cells and skin fibroblasts. Rat HS cells were isolated by digestion with pronase-collagenase followed by centrifugation in a Nycodenz gradient, as described previously[45]. The cells were then cultured in DMEM containing 10% FBS, 100 U/ml penicillin and 100 μg/ml streptomycin. After 2 d, cell debris and nonadherent cells were removed by washing and the medium was changed every 2 or 3 d thereafter. The purity was assessed by microscopy, by intrinsic vitamin A autofluorescence and by immunocytochemistry using a monoclonal antibody against desmin (1:25, Dako). Cell viability was examined by Trypan blue exclusion. Both the cell purity and viability exceeded 95%. Cells cultured for 10 d after isolation were regarded as activated HS cells[33]. Rat skin fibroblasts were obtained according to the method described previously[46].

Quantification of collagen production. Rat pHS cells or NRK cells were plated into 6-well tissue culture plates at a density of 1×10^5 per well in DMEM with 10% FBS. After 24 h culture (day 0), NRK cells were transfected with 50 nM of siRNA using Lipotrust and Rat pHS cells were treated with VA-lip-siRNAgp46 (50 nM of siRNA) or VA-lip-siRNArandom (50 nM of siRNA). On day 1, cells were washed and collagen deposited in the wells was stained with Sirius red dye (Biocolor), as previously described[13]. Unbound dye was removed by washing and the bound complex dissolved in 0.5% sodium hydroxide. Collagen was quantified by spectrophotometry at 540 nm and results were expressed as a percentage of the untreated controls.

FACS analysis of VA-lip-siRNAgp46-FAM. Rat pHS cells or primary skin fibroblast (1×10^5 cells) were treated with VA-lip-siRNAgp46-FAM (50 nM of siRNA) in the presence of various concentrations of RBP (0.07–1.4 μg/ml, SCIPAC) and were cultivated for 30 min. For the blocking assay, 1×10^5 cells were treated with mouse anti-RBP antibody (10 μg/ml, BD Pharmingen) or negative control mouse IgG1 (10 μg/ml, Dako) for 30 min before adding VA-lip-siRNAgp46-FAM. LI90 cell were treated with VA-lip-siRNAgp46-FAM in the presence of 10% FBS and were cultivated for 30 min. The MFI of VA-lip-siRNAgp46-FAM–treated cells was assessed on a FACScalibur with CellQuest software (Becton Dickinson).

Intracellular distribution analysis of VA-lip-siRNAgp46-FAM. Rat pHS cells were plated in Lab-Tek chambered cover glasses at 1×10^4 cells/chamber. VA-lip-siRNAgp46-FAM or lip-siRNAgp46-FAM was added to cells at a final siRNA concentration of 50 nM. Cells were cultured in DMEM containing 10% FBS for 30 min, then the medium were replaced with fresh medium. At 30 min and 2 h post-treatment, the cells were washed three times with PBS and fixed with 4% paraformaldehyde for 15 min at 25 °C. After fixation, the cells were washed three times with PBS and were exposed to Prolong Gold Antifade Reagent with DAPI (Molecular Probes) for 1 min to stain nuclei. The subcellular localization of FAM-labeled siRNAgp46 was assessed using fluorescent microscopy (Keyence, BZ-8000).

Treatment of animals. Male Sprague-Dawley rats (Charles River) 4 to 5 weeks old were used. All animal procedures were approved by the Sapporo Medical College Institutional Animal Care and Use Committee. Rats were anesthetized with sodium pentobarbital (40 mg/kg body weight, intraperitoneally) and exsanguinated via the inferior vena cava.

Induction of DMN liver cirrhosis. Rats were given 1% DMN dissolved in saline (1 ml/kg body weight) intraperitoneally for 3 consecutive days per week until day 24 to induce liver cirrhosis, and in some experiments, for another 3 weeks to maintain cirrhosis[38] (**Supplementary Fig. 4**).

***In vivo* localization of VA-lip-siRNAgp46-FAM in rat liver and other organs.** DMN-treated cirrhotic rats (day 24) were injected intravenously with 1 μl/g body weight of VA-lip-siRNAgp46-FAM or lip-siRNAgp46-FAM. The injections were administered under normal pressure at a daily dose of 0.75 mg/kg siRNA given three times every other day. At 24 h after the last injection, the rats were killed by saline perfusion, and the liver and other organs (lung, spleen and retina) were harvested. Tissue specimens were immediately embedded in OCT medium and cryogenically sectioned. Sections were mounted on slides, fixed in 4% paraformaldehyde washed with PBS, permeabilized with 0.2% Triton X-100 in PBS and blocked with 1% BSA in PBS.

For the immunofluorescence study, slide-mounted liver sections were treated with monoclonal anti-α-SMA-CY3-conjugated antibody (1:400, Sigma). Other tissue sections were treated with anti-CD68 antibody (1:100,

DAKO) prelabeled with the Alexa Fluor 568 Mouse IgG_1 Labeling Kit (Molecular Probes) for 2 h at 25 °C. All slides were washed with PBS and exposed to Prolong Gold Antifade Reagent with DAPI for 1 min to stain nuclei. Multicolored fluorescent staining of tissues was analyzed by confocal laser scanning microscopy using a Radiance 2100 Rainbow (Bio-Rad) equipped with a Zeiss Axioskop 2 fluorescent microscope (Carl Zeiss MicroImaging). The fluorescence signals of liver sections were video-digitized and analyzed with a software program that automatically outlined the total stained areas with threshold settings (Photoshop 4.0; Adobe). These areas were then quantified with NIH Image 1.62 software, and the transduction efficiency was calculated from the ratio of the merged yellow color area to the total α-SMA-stained area in each section. The areas were assessed in ten randomly selected high-power fields (× 630) per specimen from each liver.

VA-lip-siRNAgp46-Cy5 delivery to different cell types in the liver. DMN-treated cirrhotic rats (day 24) were injected intravenously with VA-lip-siRNAgp46-Cy5 or lip-siRNAgp46-Cy5. The injections were administered under normal pressure in a volume of 1 μl/g body weight at a daily dose of 0.75 mg/kg siRNA given 3 times, every other day. At 24 h after the last injection, HS cells, Kupffer cells, and hepatocyte-rich fractions of rat livers were obtained by the pronase-collagenase method[47] and stained with anti-α-SMA FITC (Sigma), anti-rat CD168-FITC (Serotec) and anti-rat albumin-FITC (Cedarlane Laboratories), respectively. To detect intracellular albumin and α-SMA, cells were pretreated with Perm Buffer I (BD Biosciences). Cells were then analyzed by flow cytometry.

Tissue distribution and pharmacokinetics of radiolabeled VA-lip-siRNAgp46. Radiolabeled VA-lip-siRNAgp46 was prepared by incorporating[^{3}H]retinol ([11,12-^{3}H (N)]: 44.4Ci/mmol, Perkin Elmer) into liposomes as described above for preparation of VA-coupled liposomes carrying siRNAgp46. [^{3}H]VA-lip-siRNAgp46 (200 μCi) was administered via the tail vein under normal pressure in either DMN-treated cirrhotic rats (day 24) or normal rats and blood was collected via tail vein nick over a 24-h period. After 24 h, the rats were killed under anesthesia, the tissues were harvested, and 50-mg samples were transferred to glass scintillation vials and solubilized with Solvable (Perkin Elmer). Solubilized tissues were assayed for radioactivity by liquid scintillation counting with Hionic-Fluor (Perkin Elmer).

Quantitative RT-PCR. Total RNA was isolated using RNeasy mini kit (Qiagen) according to the manufacturer's protocol. Total RNA (1 μg) were used for reverse transcription in total volume of 20 μl with the cDNA cycle kit (Invitrogen). All TaqMan primers mixed with probes were purchased from Applied Biosystems. Primers for the experiment were as follows: gp46 forward 5′-TTTAAGCCGCACTGGGATGAGAAGT-3′, reverse 5′-TGGGGACACCT TAGCATC-3′; procollagen, type I, alpha 1 (COL1A1), forward 5′-TAAGGGT GACAGAGGTGATGCTGGT-3′, reverse 5′-TGGGGACACCTTAGCATC-3′; tissue inhibitor of metalloproteinase 1 forward 5′-ACTCGGACCTGGTTA TAAGGGCTAA-3′, reverse 5′-TGGGGACACCTTAGCATC-3′; IFN-α forward 5′-AGAGCAGAAGTGTGGAGAGCCCTGT-3′, reverse 5′- ACAGGGCTCTC CACACTTCTGCTCT-3′; GAPDH, forward 5′-AACCCATCACCATCTTCCAG GAGCG-3′, reverse 5′-CATCGAAGGTGGAAGAGTGG-3′. GAPDH was used as a control for RNA integrity. The TaqMan reactions were performed using an ABI Prism 7700 sequence detection system (Applied Biosystems). The results were expressed as the ratio of the number of copies of the product gene to the number of copies of the housekeeping gene (GAPDH) from the same RNA (respective cDNA) sample and PCR run.

***In vivo* siRNAgp46 treatment.** To evaluate the effect of siRNAgp46 treatment on liver cirrhosis, we conducted two sets of experiments. In the first set of experiments, 24 groups of rats were used to determine the dose- and duration-dependent effect on survival. From day 24 of DMN administration, when serious liver cirrhosis was established (**Supplementary Fig. 4**), four treatment groups of rats were injected intravenously with VA-lip-siRNAgp46 at siRNA doses of 0.1, 0.5 or 0.75 mg/kg twice a week ($n = 6$ for each group), or 0.75 mg/kg three times a week ($n = 12$ for each group).

The 20 control groups received injections of lip-siRNAgp46, VA-lip-siRNA random, vitamin A–coupled liposome, vitamin A or PBS using the same dosage schedule as the corresponding four treatment groups. In addition, injections of siRNAgp46 (0.75 mg/kg three times a week) were also performed ($n = 12$).

In a second set of experiments, six groups of rats ($n = 12$ for each group) were used for histological and liver function evaluations. Each group was treated with PBS, vitamin A alone, vitamin A–coupled liposome, lip-siRNAgp46, VA-lip-siRNArandom or VA-lip-siRNAgp46 (0.75 mg/kg siRNA) three times a week. All injections were given via the tail vein under normal pressure in a volume of 1 μl/g body weight. The livers of rats were fixed in 10% paraformaldehyde, and paraffin-embedded sections were stained with Azan-Mallory stain or with anti-collagen I antibody (1:100, Abcam) using the EnVision system (Dako), according to the manufacturer's instructions, followed by the DakoLiquid DAB (diaminobenzidine) Substrate-Chromagen System kit.

To accurately quantify collagen I-positive areas, slides from six randomly selected low-power fields (×100) per liver section of each rat were viewed by microscopy (Axioplan 2; Carl Zeiss, Inc.). Digital pictures were captured through a video archival system using a digital TV camera system (AxioCam High Resolution color, Carl Zeiss, Inc.). An automated software analysis program (KS400, Carl Zeiss, Inc.) was used to determine the percentage of stained areas in the digital photomicrographs.

For the immunofluorescence study, slide-mounted liver sections were treated with anti-gp46 antibody (1:250, Stressgen) prelabeled using an Alexa Fluor 568 Mouse IgG_{2b} Labeling Kit (Molecular Probes). When rats were killed, blood samples were also drawn and assessed for serum bilirubin, hyaluronate, albumin and ALT by standard procedures. For assessment of histological staging, a semiquantitative scoring (scores 0 to 6) was performed as described previously[48] by an independent hepatologist (Board Certified Hepatologist of the Japan Society of Hepatology) in a blind fashion using liver preparations from 12 rats from each group.

Hydroxyproline content assay. Hydroxyproline content was determined by the Jamall methods as previously reported[49]. Briefly, liver tissue (300 mg) was homogenized in 6N HCl and hydrolyzed at 110 °C for 18 h. Twenty-five microliter aliquots were dried at 60 °C. The sediment was dissolved in 1.2 ml of 50% isopropanol and incubated with 200 ml of 0.56% chloramine T Solution (Sigma) in acetate citrate buffer pH 6.0. After incubation for 10 min at 25 °C, 1 ml of Ehrlich's reagent was added and the mixture was incubated at 50 °C for 90 min. After cooling, the absorbance was measured at 560 nm.

VA-lip-siRNAgp46 treatment of CCl_4-induced rat liver fibrosis. Liver cirrhosis was generated by 8-week treatment of adult male Sprague–Dawley (200 g) rats with CCl_4 (CCl_4 in olive oil, 1:1 (vol/vol) per kg body weight by intraperitoneal injection twice weekly) as previously described[4]. At day 58 of CCl_4 treatment, rats were treated with VA-lip-siRNAgp46, VA-lip-siRNArandom (0.75 mg/kg siRNA, two times a week) or PBS alone 2 times a week. At day 76 of CCl_4 treatment, all rats were killed and liver and serum samples were prepared. Immunohistochemical evaluations, liver function evaluations and hydroxyproline content assay were performed essentially as described in the previous section.

VA-lip-siRNAgp46 treatment of BDL-induced rat liver fibrosis. Biliary hepatic fibrosis was induced by ligation of the common bile duct of male Sprague–Dawley (200 g) rats as previously described[16]. In brief, the common bile duct was identified and double ligated with 3-0 silk ligatures. Five weeks after BDL, rats were assigned to 1 of 3 treatment groups: (i) VA-lip-siRNAgp46, (ii) VA-lip-siRNArandom or (iii) PBS alone. The injections were administered under normal pressure in a volume of 1 μl/g body weight at a daily dose of 0.75 mg/kg siRNA given five times every other day followed by six times twice a week. At day 45 and 67 of BDL, rats ($n = 10$ per group) were killed and liver and serum samples were prepared for immunohistochemical evaluations, liver function evaluations and hydroxyproline content assay as described in the previous section.

Statistics. Results are presented as means (± s.d.) for each sample. Multiple comparisons between control groups and other groups were performed by Dunnnet's test. Survival curves were constructed according to the Kaplan-Meier method and tested by Breslow-Gehan-Wilcoxon analysis.

Note: Supplementary information is available on the Nature Biotechnology website.

ACKNOWLEDGMENTS
This work was supported by grants-in-aid from Japan Society for the Promotion of Science to Y.S.

AUTHOR CONTRIBUTIONS
Y.S., K. Murase and J.K. designed research, performed experiments and wrote the paper. M.K., T.S., Y.K., R.T., K.T., K. Miyanishi, T.M. and T.T. performed experiments. Y.N. designed research, wrote the paper and supervised the whole project. All authors discussed the results and commented on the manuscript.

Published online at http://www.nature.com/naturebiotechnology/
Reprints and permissions information is available online at http://npg.nature.com/reprintsandpermissions

1. Friedman, S.L. Molecular regulation of hepatic fibrosis, an integrated cellular response to tissue injury. *J. Biol. Chem.* **275**, 2247–2250 (2000).
2. Sauk, J.J., Smith, T., Norris, K. & Ferreira, L. Hsp47 and the translation-translocation machinery cooperate in the production of alpha 1(I) chains of type I procollagen. *J. Biol. Chem.* **269**, 3941–3946 (1994).
3. Nagata, K. Expression and function of heat shock protein 47: a collagen-specific molecular chaperone in the endoplasmic reticulum. *Matrix Biol.* **16**, 379–386 (1998).
4. Issa, R. *et al.* Spontaneous recovery from micronodular cirrhosis: evidence for incomplete resolution associated with matrix cross-linking. *Gastroenterology* **126**, 1795–1808 (2004).
5. Arthur, M.J. Reversibility of liver fibrosis and cirrhosis following treatment for hepatitis C. *Gastroenterology* **122**, 1525–1528 (2002).
6. Ueki, T. *et al.* Hepatocyte growth factor gene therapy of liver cirrhosis in rats. *Nat. Med.* **5**, 226–230 (1999).
7. Parsons, C.J. *et al.* Antifibrotic effects of a tissue inhibitor of metalloproteinase-1 antibody on established liver fibrosis in rats. *Hepatology* **40**, 1106–1115 (2004).
8. Masuda, H., Fukumoto, M., Hirayoshi, K. & Nagata, K. Coexpression of the collagen-binding stress protein HSP47 gene and the alpha 1(I) and alpha 1(III) collagen genes in carbon tetrachloride-induced rat liver fibrosis. *J. Clin. Invest.* **94**, 2481–2488 (1994).
9. Nagai, N. *et al.* Embryonic lethality of molecular chaperone hsp47 knockout mice is associated with defects in collagen biosynthesis. *J. Cell Biol.* **150**, 1499–1506 (2000).
10. Bachem, M.G. *et al.* Identification, culture, and characterization of pancreatic stellate cells in rats and humans. *Gastroenterology* **115**, 421–432 (1998).
11. Fuja, T.J., Probst-Fuja, M.N. & Titze, I.R. Changes in expression of extracellular matrix genes, fibrogenic factors, and actin cytoskeletal organization in retinol treated and untreated vocal fold stellate cells. *Matrix Biol.* **25**, 59–67 (2006).
12. Roberts, A.B. *et al.* Transforming growth factor type beta: rapid induction of fibrosis and angiogenesis *in vivo* and stimulation of collagen formation *in vitro*. *Proc. Natl. Acad. Sci. USA* **83**, 4167–4171 (1986).
13. Williams, E.J. *et al.* Relaxin inhibits effective collagen deposition by cultured hepatic stellate cells and decreases rat liver fibrosis *in vivo*. *Gut* **49**, 577–583 (2001).
14. Murakami, K. *et al.* Establishment of a new human cell line, LI90, exhibiting characteristics of hepatic Ito (fat-storing) cells. *Lab. Invest.* **72**, 731–739 (1995).
15. Judge, A.D. *et al.* Sequence-dependent stimulation of the mammalian innate immune response by synthetic siRNA. *Nat. Biotechnol.* **23**, 457–462 (2005).
16. Gerling, B., Becker, M., Waldschmidt, J., Rehmann, M. & Schuppan, D. Elevated serum aminoterminal procollagen type-III-peptide parallels collagen accumulation in rats with secondary biliary fibrosis. *J. Hepatol.* **25**, 79–84 (1996).
17. Bataller, R. & Brenner, D.A. Liver fibrosis. *J. Clin. Invest.* **115**, 209–218 (2005).
18. Jackson, A.L. *et al.* Expression profiling reveals off-target gene regulation by RNAi. *Nat. Biotechnol.* **21**, 635–637 (2003).
19. Marques, J.T. *et al.* A structural basis for discriminating between self and nonself double-stranded RNAs in mammalian cells. *Nat. Biotechnol.* **24**, 559–565 (2006).
20. Kim, D.H. *et al.* Interferon induction by siRNAs and ssRNAs synthesized by phage polymerase. *Nat. Biotechnol.* **22**, 321–325 (2004).
21. Kim, D.H. *et al.* Synthetic dsRNA Dicer substrates enhance RNAi potency and efficacy. *Nat. Biotechnol.* **23**, 222–226 (2005).
22. Bartlett, D.W. & Davis, M.E. Insights into the kinetics of siRNA-mediated gene silencing from live-cell and live-animal bioluminescent imaging. *Nucleic Acids Res.* **34**, 322–333 (2006).
23. Zimmermann, T.S. *et al.* RNAi-mediated gene silencing in non-human primates. *Nature* **441**, 111–114 (2006).
24. Yano, J. *et al.* Antitumor activity of small interfering RNA/cationic liposome complex in mouse models of cancer. *Clin. Cancer Res.* **10**, 7721–7726 (2004).
25. Song, E. *et al.* RNA interference targeting Fas protects mice from fulminant hepatitis. *Nat. Med.* **9**, 347–351 (2003).
26. Flower, D.R. Beyond the superfamily: the lipocalin receptors. *Biochim. Biophys. Acta* **1482**, 327–336 (2000).
27. Blomhoff, R., Berg, T. & Norum, K.R. Transfer of retinol from parenchymal to stellate cells in liver is mediated by retinol-binding protein. *Proc. Natl. Acad. Sci. USA* **85**, 3455–3458 (1988).
28. Senoo, H. *et al.* Internalization of retinol-binding protein in parenchymal and stellate cells of rat liver. *J. Lipid Res.* **31**, 1229–1239 (1990).
29. Senoo, H. *et al.* Transfer of retinol-binding protein from HepG2 human hepatoma cells to cocultured rat stellate cells. *Proc. Natl. Acad. Sci. USA* **90**, 3616–3620 (1993).
30. Fortuna, V.A., Martucci, R.B., Trugo, L.C. & Borojevic, R. Hepatic stellate cells uptake of retinol associated with retinol-binding protein or with bovine serum albumin. *J. Cell. Biochem.* **90**, 792–805 (2003).
31. Noy, N. & Xu, Z.J. Kinetic parameters of the interactions of retinol with lipid bilayers. *Biochemistry* **29**, 3883–3888 (1990).
32. Blomhoff, R. & Wake, K. Perisinusoidal stellate cells of the liver: important roles in retinol metabolism and fibrosis. *FASEB J.* **5**, 271–277 (1991).
33. Rockey, D.C., Boyles, J.K., Gabbiani, G. & Friedman, S.L. Rat hepatic lipocytes express smooth muscle actin upon activation *in vivo* and in culture. *J. Submicrosc. Cytol. Pathol.* **24**, 193–203 (1992).
34. Osaka, G. *et al.* Pharmacokinetics, tissue distribution, and expression efficiency of plasmid DNA following intravenous administration of DNA/cationic lipid complexes in mice: Use of a novel radionuclide approach. *J. Pharm. Sci.* **85**, 612–618 (1996).
35. Walsh, T.J. *et al.* Liposomal amphotericin B for empirical therapy in patients with persistent fever and neutropenia. National Institute of Allergy and Infectious Diseases Mycoses Study Group. *N. Engl. J. Med.* **340**, 764–771 (1999).
36. Takahashi, N., Tamagawa, K., Shimizu, K., Fukui, T. & Maitani, Y. Effects on M5076-hepatic metastasis of retinoic acid and N-(4-hydroxyphenyl) retinamide, fenretinide entrapped in SG-liposomes. *Biol. Pharm. Bull.* **26**, 1060–1063 (2003).
37. Behlke, M.A. Progress towards *in vivo* use of siRNAs. *Mol. Ther.* **13**, 644–670 (2006).
38. Jezequel, A.M. *et al.* A morphological study of the early stages of hepatic fibrosis induced by low doses of dimethylnitrosamine in the rat. *J. Hepatol.* **5**, 174–181 (1987).
39. Farber, J.L. & El-Mofty, S.K. The biochemical pathology of liver cell necrosis. *Am. J. Pathol.* **81**, 237–250 (1975).
40. Zhou, X. *et al.* Expression of matrix metalloproteinase-2 and -14 persists during early resolution of experimental liver fibrosis and might contribute to fibrolysis. *Liver Int.* **24**, 492–501 (2004).
41. Steffensen, B., Wallon, U.M. & Overall, C.M. Extracellular matrix binding properties of recombinant fibronectin type II-like modules of human 72-kDa gelatinase/type IV collagenase. High affinity binding to native type I collagen but not native type IV collagen. *J. Biol. Chem.* **270**, 11555–11566 (1995).
42. Peterkofsky, B. & Diegelmann, R. Use of a mixture of proteinase-free collagenases for the specific assay of radioactive collagen in the presence of other proteins. *Biochemistry* **10**, 988–994 (1971).
43. Kikuchi, A. *et al.* Development of novel cationic liposomes for efficient gene transfer into peritoneal disseminated tumor. *Hum. Gene Ther.* **10**, 947–955 (1999).
44. Serikawa, T., Suzuki, N., Kikuchi, H., Tanaka, K. & Kitagawa, T. A new cationic liposome for efficient gene delivery with serum into cultured human cells: a quantitative analysis using two independent fluorescent probes. *Biochim. Biophys. Acta* **1467**, 419–430 (2000).
45. Schafer, S., Zerbe, O. & Gressner, A.M. The synthesis of proteoglycans in fat-storing cells of rat liver. *Hepatology* **7**, 680–687 (1987).
46. Fargnoli, J., Kunisada, T., Fornace, A.J., Jr., Schneider, E.L. & Holbrook, N.J. Decreased expression of heat shock protein 70 mRNA and protein after heat treatment in cells of aged rats. *Proc. Natl. Acad. Sci. USA* **87**, 846–850 (1990).
47. Zhang, X. *et al.* Effects of lipopolysaccharides stimulated Kupffer cells on activation of rat hepatic stellate cells. *World J. Gastroenterol.* **10**, 610–613 (2004).
48. Ishak, K. *et al.* Histological grading and staging of chronic hepatitis. *J. Hepatol.* **22**, 696–699 (1995).
49. Jamall, I.S., Finelli, V.N. & Que Hee, S.S. A simple method to determine nanogram levels of 4-hydroxyproline in biological tissues. *Anal. Biochem.* **112**, 70–75 (1981).